

Induced Ge spin polarization at the Fe/Ge interfaceJ. W. Freeland,¹ R. H. Kodama,² M. Vedpathak,² S. C. Erwin,³ D. J. Keavney,¹ R. Winarski,¹ P. Ryan,¹ and R. A. Rosenberg¹¹*Advanced Photon Source, Argonne National Laboratory, Argonne, Illinois 60439, USA*²*Department of Physics, University of Illinois at Chicago, Chicago, Illinois 60607, USA*³*Center for Computational Materials Science, Naval Research Laboratory, Washington, DC 20375, USA*

(Received 12 March 2004; published 7 July 2004)

We report direct experimental evidence showing induced magnetic moments on Ge at the interface in an Fe/Ge system. Details of the x-ray magnetic circular dichroism and resonant magnetic scattering at the Ge *L* edge demonstrate the presence of spin-polarized *s* states at the Fermi level, as well as *d*-character moments at higher energy, which are both oriented antiparallel to the moment of the Fe layer. Use of the sum rules enables extraction of the *L/S* ratio, which is zero for the *s* part and ~ 0.5 for the *d* component. These results are consistent with layer-resolved electronic structure calculations, which estimate that the *s* and *d* components of the Ge moment are antiparallel to the Fe 3*d* moment and have a magnitude of $\sim 0.01 \mu_B$.

DOI: 10.1103/PhysRevB.70.033201

PACS number(s): 75.70.Cn, 78.70.Dm, 79.60.Jv

Understanding the transport of spins across the ferromagnet/semiconductor interface poses many fundamental questions but has wide implications for spin-based electronics.¹ A key area is understanding how spin polarized electrons or holes are injected from a magnetic material into a semiconductor.^{2,3} If the spins are injected from a ferromagnet then one needs to consider the influence of the magnetic component on the semiconductor electronic structure. Induced moments have been observed in all metal ferromagnet/nonmagnet systems,⁴⁻⁶ but never directly in the ferromagnet/semiconductor system. Electronic structure calculations have predicted an induced moment ($\sim 0.1 \mu_B$) and modified density of states at the boundary,⁷⁻⁹ but there is a lack of direct evidence for these induced interface moments.

In this Brief Report we present direct evidence of spin-polarized Ge at the interface with a magnetic transition metal. X-ray magnetic circular dichroism at the Ge *L* edge in an Fe/Ge multilayer provided unambiguous evidence for induced spin on Ge. A comparison with single crystal results enables the identification of the spin polarization into a *s* moment close to the Fermi level and a *d* component at higher energy. The data are consistent with an antiparallel induced moment on Ge with indications of a nonzero orbital moment for the *d* component. Layer-resolved electronic structure calculations show the induced moment is localized around the interface with the *s* and *d* moments $\sim 0.01 \mu_B$ that are antiparallel to the Fe 3*d* moment.

Element-selective magnetic measurements were made using an x-ray magnetic circular dichroism (XMCD),¹⁰ which arises from the coupling of the magnetic orientation to the x-ray polarization. These experiments were performed at sector 4 of the Advanced Photon Source.¹¹ Beamline 4-ID-C provides high-resolution polarized x-rays in the intermediate x-ray range of 500–3000 eV. The x-rays are generated by a novel circularly polarized undulator that provides left- and right-circular polarization switchable on demand at a polarization $>96\%$. The samples were studied by the measurement of total fluorescence yield (TFY) using a microchannel plate detector. Fluorescence yield was used both because of its bulk sensitivity, as well as the ability to measure in an

applied magnetic field. The measurement involves changing the magnetization direction at each energy point of the absorption curve to measure the absorption with photon helicity and magnetization parallel (I^+) and antiparallel (I^-). The sum ($I^+ + I^-$) provides chemical information while the XMCD ($I^+ - I^-$) is magnetic in origin. Since the XMCD signal is very small, it was confirmed that the XMCD changed sign upon reversal of the photon helicity.

To maximize the interface contribution to the absorption signal, a multilayer sample was used. The Fe/Ge multilayers were prepared by sputtering at room temperature with a nominal structure of Si(100)/Ge(100 Å)/[Fe(22 Å)/Ge(22 Å)]₂₀/Ge(100 Å) as confirmed by x-ray reflectivity and TEM. It should be noted here that Ge grown on Fe results in an amorphous structure while the Fe is polycrystalline.¹² Since measurements of amorphous Ge indicate that the nearest neighbor spacing is close to the crystalline case,¹³ each monolayer (ML) will correspond to ~ 2 Å from which it can be estimated that the interface comprises approximately 10% of the sample. One issue of concern is alloying at the Fe/Ge interface, which has been observed at Fe/Ge interfaces.¹⁴ This issue will be addressed in more detail below when we demonstrate that the results here are consistent with an abrupt Fe/Ge component even though intermixing is present in the Fe/Ge system.

Measurement of the polarization-dependent absorption at the Ge *L* edge (see Fig. 1) provides direct access to the electronic and magnetic order of Ge. Due to the dipole selection rules for x-ray absorption, this excitation details the *d* and *s* contributions to the spin polarized density of unoccupied states. The presence of a nonzero XMCD provides direct evidence of the spin-polarized Ge, but a more detailed analysis of the data requires an understanding of the electronic character of the unoccupied states contributing to the XMCD. As will be shown below, the XMCD can be considered as consisting of 3 fundamental components: a negative peak close to the Fermi level ascribed to spin-polarized *s* states, higher lying spin-polarized *d* states, and an extended component that may be attributed to a magnetic extended absorption fine structure.¹⁵ To assign the XMCD to particular

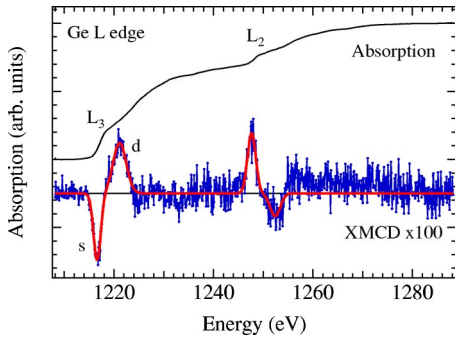


FIG. 1. (Color online) Average absorption ($I^+ + I^-$) and x-ray magnetic circular dichroism [$\text{XMCD} = (I^+ - I^-)$] at the Ge L edge for the Fe/amorphous Ge multilayer. Nonzero XMCD gives a clear indication of an induced magnetic moment on Ge. The structure in the XMCD is attributed to both spin-polarized s and d states, as well as a small magnetic signal in the extended signal, which might be due to a magnetic extended absorption fine structure. The red line is a Gaussian fit to the data discussed in the text.

electronic states first consider the results for bulk Ge, which will provide an initial framework.

Calculations for amorphous Ge (a -Ge) show the density of unoccupied states is nearly the same as crystalline (c -Ge) with only small modifications.¹⁶ The peaks in the c -Ge case result both from the s and d density of unoccupied states as well as multiple scattering from the highly ordered crystal.¹⁷ The edge for the c -Ge case was described by an initial peak due to s states followed by a double-peak feature due to d states. Results for the a -Ge system could be reproduced by the same density of states simply by varying the degree of coherent multiple scattering to simulate the disordered amorphous state.¹⁷ A comparison of the Fe/Ge absorption results with a single crystal Ge(100) wafer is shown in Fig. 2 and agrees well with the previous study of the x-ray absorption of a -Ge. Using this result enables an initial assignment based on the bulk electronic structure. The first XMCD peak (labeled s in Fig. 2) lies in the pre-edge region close to the Fermi level (solid line in Fig. 2), which may have an important impact on spin-dependent transport. The

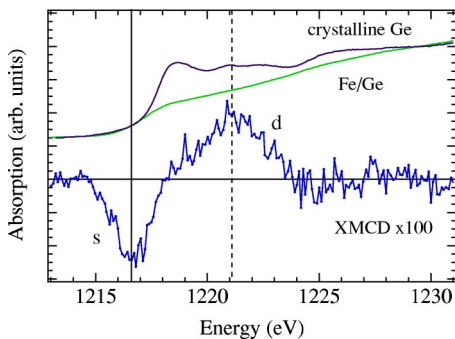


FIG. 2. (Color online) A comparison of Ge L_3 absorption for the Fe/Ge sample and a single-crystal Ge standard. Note the distinct drop in the absorption for the Fe/Ge case, which is associated with the disorder of the amorphous state. Vertical lines indicate the alignment of XMCD features with features ascribed to s and d states in the absorption.

bulk electronic structure in this region is predominantly s character. The second XMCD peak coincides with the doublet assigned to d states (labeled d in Fig. 2). This provides an initial assignment as shown in Fig. 2, which is consistent with the analysis of the experimental data and the layer resolved density of state calculations, both of which are discussed below.

With an assignment of features, the dipole selection rules enable the determination of orientation between the Fe and Ge moments. The XMCD selection rules for $p \rightarrow d$ vs $p \rightarrow s$ ^{18,19} allow s and d contributions to the spin moment, $\langle S_z \rangle$, to be written as

$$\langle S_z \rangle = \langle S_z^d \rangle - 2 \langle S_z^s \rangle \frac{P_s}{P_d} + \frac{7}{2} \langle T_z \rangle, \quad (1)$$

where P_s/P_d is the probability ratio for s vs d excitation and $\langle T_z \rangle$ is the magnetic dipole term. In accord with recent results, it can be assumed that $P_s P_d \sim 1$ (Ref. 19) and $\langle T_z \rangle \approx 0$.²⁰ The important point is that the selection rules result in a minus sign between the d vs s XMCD for the same magnetic moment direction. Since the initial L_3 XMCD is negative for Fe (not shown), this is direct evidence of the antiparallel orientation of the Ge s moment and the $3d$ transition metal moment. The d component has a positive signal indicating that the d component of the induced Ge moment is antiparallel to that of Fe as well. These results are in agreement with the electronic structure calculations presented below.

The sum rule analysis provides a more detailed insight into the magnetic structure, but there are difficulties in the application to the case of Ge. Without a continuum excitation background subtraction and knowledge of the number of $4s$ and d holes in the conduction band, extraction of the spin and orbital moments is not possible. This is further complicated by the possibility of charge transfer at the interface, which will mix the $3d$ electrons from Fe with the $4d$ electrons from Ge. However, the ratio, $R_m = \Delta A_{L_3} / \Delta A_{L_2}$, where ΔA_L is the area of the respective XMCD peak, can provide the ratio of spin to an orbital moment. Due to the small signal to noise in the spectrum, the peaks were fit with Gaussians, and the fit data were used for the energy integration (see Fig. 1). With a small signal to noise, the result can be led astray by noise contributions. Since the purpose is to determine general trends in the spin-orbit ratio, the fit works very well and allows the two contributions to be separated, assuming no overlap of the relative features.

From the area of the separate components, we can determine the orbit to spin ratio defined as

$$\langle L_z \rangle / \langle S_z \rangle \sim \frac{4 R_m + 1}{3 R_m - 2}. \quad (2)$$

In this case we have not included factors for the different character of the states. The results are shown in Table I. The numbers for $\langle L_z \rangle / \langle S_z \rangle$ provide an additional confirmation of the character assignment. The s component results in an $\langle L_z \rangle \sim 0$, and the second peak in the XMCD results in a nonzero $\langle L_z \rangle$ consistent with a d component. It is worth noting that the orbital moment is a significant fraction of the total

TABLE I. Results of sum rule analysis for the fit to the data shown in Fig. 1.

State	R_m	$\langle L_z \rangle / \langle S_z \rangle$
s	-0.98	-0.01(10)
d	-2.85	0.5(1)

moment and perhaps plays a role in the uniaxial part of the anisotropy for Fe/Ge(100).²¹ We will show below the d moment is $0.01 \mu_B$, which results in an orbital moment $0.005 \mu_B$. The magnitude of this orbital component is consistent with theoretical results ascribing the observed uniaxial anisotropy to nonzero moments in the semiconductor.⁸

To interpret these results theoretically, we turn to density-functional theory calculations. Two sets of calculations were performed to elucidate different aspects of induced Ge moments in Fe: (1) an ideal interface and an intermixed interface, and (2) fixed-spin-moment calculations for bulk Ge, for the purpose of estimating the ratio between induced p -moments (which are the largest) to s and d moments (which are measured by the L edge XMCD). The calculations were performed within the generalized-gradient approximation, using projector-augmented-wave potentials.^{22,23} The plane-wave cutoff and k -point sampling were sufficient to converge all quantities to the precision given.

To study Fe/Ge interfaces, we used two models introduced previously for Fe/GeAs interfaces.⁹ All are 1×1 interfaces between crystalline Ge and Fe, with the interface boundary either ideal (i.e., atomically abrupt) or rough (with 1.0 monolayers of Ge in the Fe host). The isolated interfaces were modeled by supercells containing seven layers each of Ge and Fe, with atomic coordinates completely relaxed within two layers of the interface. The induced Ge moments for both structures are shown in Fig. 3; the results for the other two models are qualitatively similar. The interfacial Ge layer has a moment of $0.06 \mu_B$ antiparallel to the Fe magnetization. Although small, this is roughly half the value obtained for isolated Ge in an Fe matrix and thus appears reasonable. Ge atoms one layer away from the interface are less polarized (in the Fe direction), and further layers are essen-

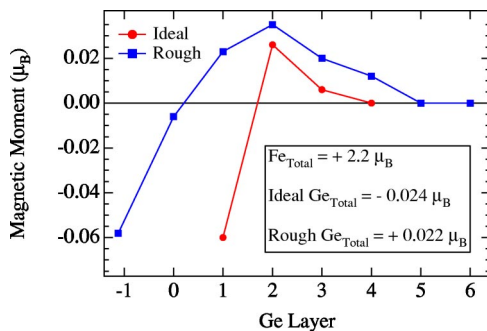


FIG. 3. (Color online) Layer-resolved calculated moments for an ideal and rough Fe/Ge interface. The inset shows the average total moment for the structure, since XMCD in absorption is an average over all layers that contribute a magnetic signal.

tially nonmagnetic. The Ge moments near the interface are predominantly p -like. In comparison with the metallic case,⁴⁻⁶ it is worth noting that the layer dependence shows a similar oscillation except the oscillation is damped to zero within a few layers (see Fig. 3). For the case of a metal, the oscillation is due to a polarization of conduction electrons at the Fermi level. In a bulk semiconductor there is no density of states at the Fermi level, but near the Fe/Ge interface there is a nonzero density of states at E_f which disappears 3 layers into Ge and results in a damping of the induced Ge magnetic moment.

However, the L -edge XMCD is only sensitive to the s and d components of the total Ge moment. For the calculations described above, these contributions were only $\sim 10\%$ of the already small total Ge moment and hence are numerically difficult to resolve. To determine these ratios more systematically, we performed fixed-spin-moment calculations for crystalline Ge, varying the total moment, M , from zero to $1.5 \mu_B$. For each value of M , we computed the s , p , and d contributions within an atomic sphere. The ratios M_s/M_p and M_d/M_p are remarkably independent of the total moment. They do, however, depend strongly on the sphere radius used: for touching spheres $M_s/M_p=0.3$ and $M_d/M_p=0.1$, while for volume-filling spheres $M_s/M_p=0.1$ and $M_d/M_p=0.3$. Most importantly, the s - and d -moments are always parallel to the p -moment.

Using the fact that $M_{s,d} \sim 0.2M_p$, it can be inferred that the induced s - and d -moments on Ge atoms near the Fe/Ge interface are $\sim 0.01 \mu_B$. There is also a consistency between the average moment orientation and the experimental results showing anti-alignment of the Ge s - and d -moments with respect to the Fe $3d$ moment. Together with the result that the average moment for the simple alloy case is parallel to the Fe $3d$ moment with about the same magnitude, one can see that in a system with abrupt and alloyed regions might result in a cancellation of the XMCD effect. A recent study claims that this system cannot be considered simply as an abrupt Fe/Ge interface,¹⁴ but is described by intermixing that seems to occur in a strange fashion. The Ge/Fe interfaces are somewhat abrupt while the Fe/Ge interfaces seem to consist of coexisting abrupt and alloyed regions. From the details of

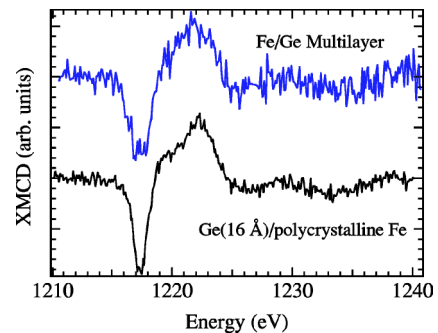


FIG. 4. (Color online) A comparison of XMCD from an Fe/Ge multilayer and a 16 \AA Ge film grown *in situ* on polycrystalline Fe. Within the noise, the two spectra are identical. Since the latter shows the minimal alloying of Fe, this is a good indication that the magnetic component resides at an Fe/Ge interface and is not due to an Fe-Ge alloy phase.

this study we can estimate that the alloy component would comprise at most 25% of the sample. To confirm our result and rule out the possibility of this magnetic phase being ascribed to an alloy, an amorphous Ge thin film was prepared *in situ* on a clean polycrystalline Fe surface.

Utilizing the idea that the Ge on Fe growth forms a relatively abrupt interface, we prepared a sample *in-situ* under UHV conditions with the following structure: Si/polycrystalline Fe(50 Å)/amorphous Ge(16 Å). X-ray photoelectron spectroscopy (XPS) showed the sample was free from contamination and there was minimal intermixing of Fe and Ge. The shape of the Ge 3*d* core level is extremely sensitive to alloy formation²⁴ and no change was observed indicating no alloy formation. As shown in Fig. 4, the measured XMCD spectra of the single Ge layer and the Fe/Ge multilayer are identical, which proves that the moment is

formed at the Fe/Ge interface and not due to an Fe_xGe_{1-x} phase.

In conclusion, element-resolved magnetic measurements have provided direct evidence for the formation of induced magnetic moments on Ge at the Fe/Ge interface. An analysis of the XMCD data is consistent with the LSDA calculations for magnitude and direction of the Ge induced moments. Future work will focus on these single-layer structures to extract a more detailed understanding of the interface electronic and magnetic structure, together with a connection to spin-dependent transport.

Use of the Advanced Photon Source was supported by the U.S. Department of Energy, Office of Science, under Contract No. W-31-109-Eng-38. Computations were performed at the DoD Major Shared Resource Centers at ASC. This work was supported in part by the Office of Naval Research.

-
- ¹S. A. Wolf, D. D. Awschalom, R. A. Buhrman, J. M. Daughton, S. von Molnar, M. L. Roukes, A. Y. Chtchelkanova, and D. M. Treger, *Science* **294**, 1488 (2001).
- ²R. Fiederling, M. Keim, G. Reuscher, W. Ossau, G. Schmidt, A. Waag, and L. W. Molenkamp, *Nature (London)* **402**, 787 (1999).
- ³Y. Ohno, D. K. Young, B. Beschoten, F. Matsukura, H. Ohno, and D. D. Awschalom, *Nature (London)* **402**, 790 (1999).
- ⁴M. Samant, J. Stöhr, S. Parkin, G. Held, B. Hermsmeier, F. Herman, M. van Schilfgaarde, L. Duda, D. Mancini, N. Wassdahl, and R. Nakajima, *Phys. Rev. Lett.* **72**, 1112 (1994).
- ⁵S. Pizzini, A. Fontaine, C. Giorgetti, E. Dartyge, J. Bobo, M. Piecuch, and F. Baudelet, *Phys. Rev. Lett.* **74**, 170 (1995).
- ⁶G. R. Harp, S. S. P. Parkin, W. L. O'Brien, and B. P. Tonner, *Phys. Rev. B* **51**, 12037 (1995).
- ⁷W. E. Pickett and D. A. Papaconstantopoulos, *Phys. Rev. B* **34**, 8372 (1986).
- ⁸I. Cabria, A. Y. Perlov, and H. Ebert, *Phys. Rev. B* **63**, 104424 (2001).
- ⁹S. C. Erwin, S.-H. Lee, and M. Scheffler, *Phys. Rev. B* **65**, 205422 (2002).
- ¹⁰C. T. Chen, Y. U. Idzerda, H.-J. Lin, N. V. Smith, G. Meigs, E. Chaban, G. H. Ho, E. Pellegrin, and F. Sette, *Phys. Rev. Lett.* **75**, 152 (1995).
- ¹¹J. W. Freeland, J. C. Lang, G. Srajer, R. Winarski, D. Shu, and D. M. Mills, *Rev. Sci. Instrum.* **73**, 1408 (2001).
- ¹²C. Majkrzak, J. Axe, and P. Böni, *J. Appl. Phys.* **57**, 3657 (1985).
- ¹³M. A. Paesler, D. E. Sayers, R. Tsu, and J. Gonzalez-Hernandez, *Phys. Rev. B* **28**, 4550 (1983).
- ¹⁴M. Schleberger, P. Walser, M. Hunziker, and M. Landolt, *Phys. Rev. B* **60**, 14360 (1999).
- ¹⁵G. Schütz, W. Wagner, W. Wilhelm, P. Kienle, R. Zeller, R. Frahm, and G. Materlik, *Phys. Rev. Lett.* **58**, 737 (1987).
- ¹⁶D. E. Rodrigues and J. F. Weisz, *Phys. Rev. B* **36**, 6685 (1987).
- ¹⁷P. Castrucci, R. Gunnella, M. De Crescenzi, M. Sacchi, G. Dufour, and F. Rochet, *Phys. Rev. B* **60**, 5759 (1999).
- ¹⁸W. L. O'Brien and B. P. Tonner, *Phys. Rev. B* **50**, 12672 (1994).
- ¹⁹S. S. Dhesi, H. A. Dürr, G. van der Laan, E. Dudzik, and N. B. Brookes, *Phys. Rev. B* **60**, 12852 (1999).
- ²⁰J. Stöhr and H. König, *Phys. Rev. Lett.* **75**, 3748 (1995).
- ²¹P. Ma and P. R. Norton, *Phys. Rev. B* **56**, 9881 (1997).
- ²²G. Kresse and J. Hafner, *Phys. Rev. B* **47**, 558 (1993).
- ²³G. Kresse and J. Fürthmüller, *Phys. Rev. B* **54**, 11169 (1996).
- ²⁴M. del Giudice, J. J. Joyce, and J. H. Weaver, *Phys. Rev. B* **36**, 4761 (1987).